Lasers in Manufacturing Conference 2021

3D printing of Al-Li with increased Li content using laser assisted powder bed fusion

Burak Yürekli[a, *], Dongmei Liu[b], Tobias Ullsperger[a], Hagen Kohl[a], Lisa Schade[a], Gabor Matthäus[a], Markus Rettenmayr[b], Stefan Nolte[a,c]

[a] *Institute of Applied Physics, Abbe Center of Photonics, Friedrich Schiller University Jena, Albert-Einstein-Straße 15, 07745 Jena, Germany*
[b] *Otto Schott Institute of Material Research, Friedrich-Schiller-Universität Jena, Löbdergraben 32, 07743 Jena, Germany*
[c] *Fraunhofer Institute for Applied Optics and Precision Engineering IOF, Center of Excellence in Photonics, Albert-Einstein-Straße 7, 07745 Jena, Germany*

Abstract

Based on the extraordinary low atomic mass of Li, Al-Li alloys hold high potential for future lightweight construction materials. In particular, the elastic modulus of Al-Li alloys increases significantly with rising Li content, offering the potential of extremely high stiffness as compared to conventional Al alloys. However, due to the formation of brittle δ-AlLi during conventional casting processes, the maximum Li content in commercial Al-Li alloys is generally limited to about 2 wt. %. Here we present laser assisted 3D printing using Al-Li alloy powders with an increased Li content of about 4 wt. %. The process is based on custom-made Al-Li powders, which is characterized in terms of powder particle size, density, absorption, and thermal conductivity. In contrast to common approaches, ultrashort laser pulses are used for the melting process, delivering 3D printed parts with a drastically reduced fraction of δ-AlLi phase due to the increased solidification rates in the melt pool.
Keywords: Additive manufacturing; Selective laser melting; Powder bed fusion; 3D printing; Aluminum–lithium alloy

1. Introduction

Additive manufacturing (AM) attracted increased attention within the scientific and industrial community over the last two decades and became an established fabrication technique [1, 2]. Laser powder bed fusion

* Corresponding author.
E-mail address: burak.yuerekli@uni-jena.de.

(LPBF) stands out as one of the renowned methods for AM of complex metal structures [3-5]. Typically, continuous wave lasers are used in LBPF; however, there is also interest in applying ultrashort pulse (USP) lasers. These lasers are widely used in micro machining due to the very short interaction time between radiation and matter, and therefore, thermal effects in the vicinity of the processed area can be significantly reduced [9, 16].

On the other hand, highly localized heat accumulation can be realized using ultrashort laser pulses at high repetition rates. When the applied fluence is chosen below the material specific ablation threshold, the absorbed laser energy is transformed into heat. This induced heat per pulse can be accumulated over times when the specific thermal diffusion of the material does not reach thermal equilibrium before the next pulse arrives. With the help of this accumulation effect, materials of high melting point can be easily melted when pulse repetition rates in the MHz are applied [6-11].

AM by using ultrashort pulsed lasers was reported for several materials like glass, copper, tungsten and aluminum alloys. Binary Al-Li alloy with high Li content is a new material featuring many extraordinary properties, especially a significantly increased elastic modulus with increasing Li content up to 4wt.% [12]. Furthermore, the density decreases with increasing Li content due to the low atomic mass of Li. However, practically, the amount of Li in Al-Li alloys is much lower, generally less than 2wt. %. When the fraction of Li within the alloy exceeds approx. 2 wt.%, brittle δ-AlLi phase form both along the grain boundaries and in the grain during conventional solidification processes of medium cooling rates, which contributes to deteriorated properties. This is the main reason why commercial Al-Li alloys are mostly available with a maximum Li content of 2 wt. %. The theoretical limit for the solubility, 4 wt. % Li, cannot be applied for rigid mechanical components as long as the formation of δ-AlLi is not suppressed [13]. One approach to avoid the precipitation of δ-AlLi is the use of extremely rapid cooling rates when USP lasers are applied during the LPBF process of Al-Li alloys.

In our previous study, we demonstrated the very first 3D printed Al-Li structures based on Al-Li alloy powders of 4 wt. % Li [14, 15] (see, Fig 1. (a)). The microstructure was significantly improved due to a reduced existence of δ-AlLi. Fig. 1. (b) and (c) shows the microstructure comparison of a conventionally cast Al- 4 wt. % Li ingot in which δ-AlLi exists along the grain boundaries (illustrated by the red circle) and inside the grain and the laser processed Al-4 wt. %. Li in which the δ-AlLi phase is significantly reduced. However, the LPBF samples exhibit high porosity mainly because of the low average laser power (25 W) of the applied USP laser system. In the present paper, LPBF of Al-Li alloys using a higher-power ultrashort pulse laser system up to 150 W has been performed, which allows the generation of Al-Li components of significantly increased density values in the range of 95%.

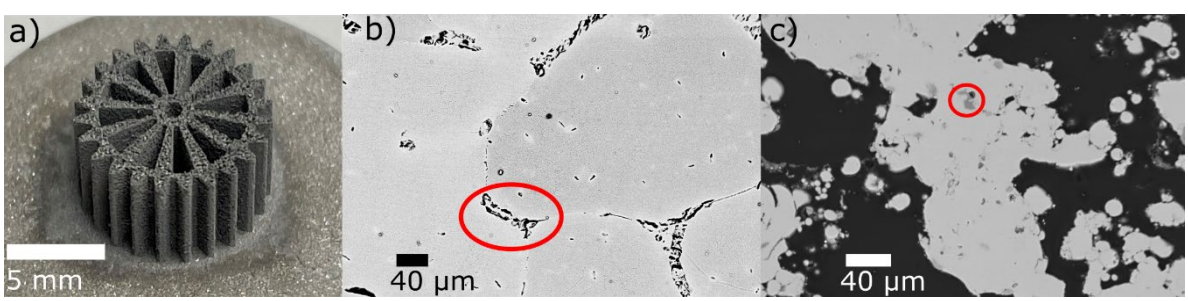

Fig 1. (a) Gear wheel as 3D printed structure (b) SEM (BSE) image of as-cast Al-Li ingot (c) SEM (BSE) image of laser-processed Al-Li.

2. Experimental Setup

Binary Al-Li powders with high Li content is not commercially available and therefore Al-Li ingots were produced in-house [14, 15]. Therefore, high purity Al and Li granulates were melted and casted under argon atmosphere. Afterwards, the contamination free ingots were delivered to the company NANOVAL where the powder fabrication by gas atomization was performed. The powder particle have a spherical shape and the particle size distribution is d_{10}= 5 µm, d_{50}= 13 µm and d_{90}= 24 µm.

During our investigations, a self-developed LPBF system in combination with an USP laser system (Active Fiber Systems) was used [15]. The main parameters are as follows: laser wavelength: 1030 nm, max. average power: 150 W, repetition rate: 40 MHz, pulse length: 300 fs and focal diameter of the laser spot on the powder surface: 46 µm. During the LPBF process, powder layers with a thickness 25 µm were applied. All experiments were performed under argon atmosphere with a residual oxygen level smaller than 0.6 %. Firstly, single-track walls with different parameter sets were built. In order to investigate a proper processing window, the repetition rate and layer thickness were kept constant, while the applied average power was varied in the range from 75 to 150 W and the processing speed between 0.1 and 0.5 m/s. The generated single wall structures had a length of 10 mm and a total height of 6 mm. Secondly, cuboid samples 6x6x6 mm^3 were prepared using the USP-LPBF. The scanning direction was rotated 90 degrees at each layer in order to assure symmetricity during process. For analyzing the microstructure of the LPBF walls, the samples were first embedded in epoxy resin, and then ground using SiC paper up to 1200 grid and polished. Then the microstructure of the top view of the LPBF walls was characterized using optical microscope (OM) and scanning electron microscope (SEM) equipped with backscattered electron (BSE) detector.

3. Experimental Results and Discussion

Single-track walls produced with different average laser powers, scanning speeds and hatching distances are shown in Fig. 2 (a). With the average laser power of 100 W, the microstructure of the walls under OM at different scanning speeds are shown Figs. 2 (b) – (f). The wall thicknesses decrease as higher scanning speed is used, because less energy is deployed during the scanning time with higher scanning speed. With the sufficient accumulated energy, continuous melting lines can be achieved, as shown in Figs. 2(b) and (c). However, the vapor in the melt pool might stuck in the material and circular holes were found within the melt lines. Lower average laser power resulted in discontinuities at walls and higher average powers may result in larger vapor holes depending on the scanning speed. Therefore, the parameter sets with 100 W and 150 W average laser power along with particular scanning speeds were chosen to build cuboid structures.

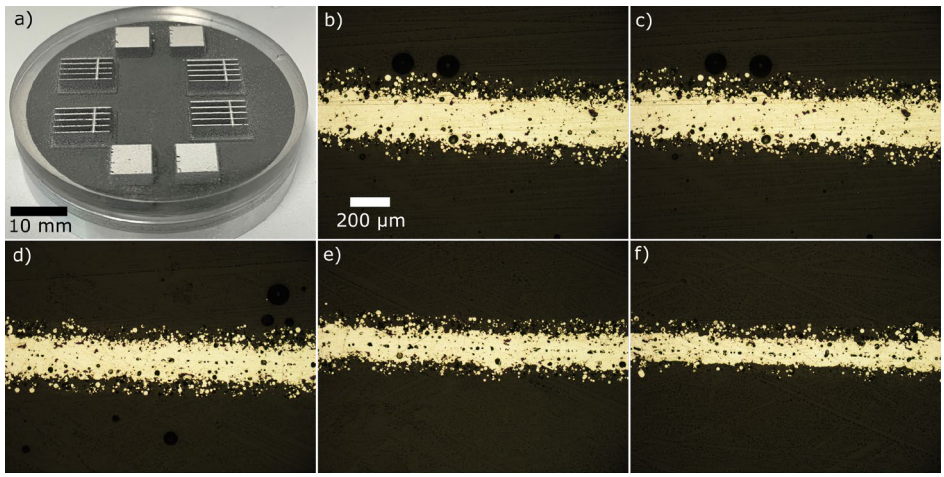

Fig. 2. (a) Photograph of the embedded and top-polished sample containing fused walls and fabricated cubes of the parameter study. Images of single-track walls generated with 100 W average power and scanning speeds of (b) 100 mm/s; (c) 200 mm/s; (d) 300 mm/s; (e) 400 mm/s; (f) 500 mm/s

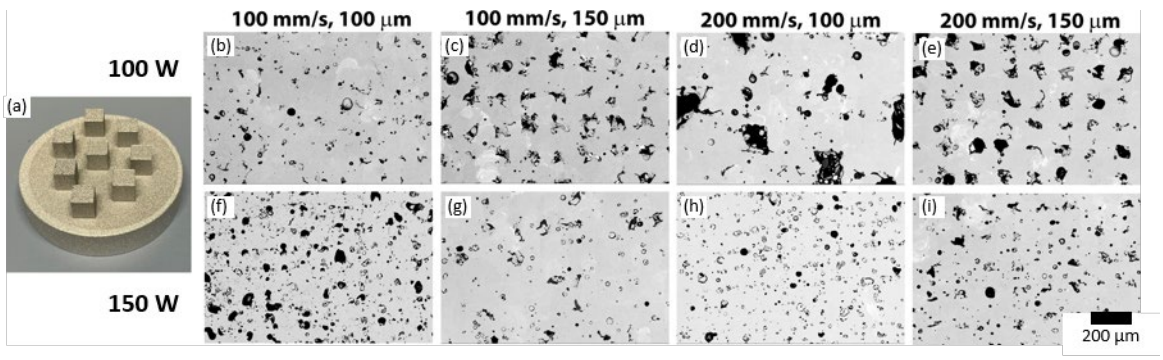

Fig. 3. (a) cuboids with dimensions of 6x6x6 mm^3; (b-i) SEM (BSE) image of a samples produced using 100 W and 150 W average power, 100 mm/s and 200 mm/s scanning speed, 100 µm and 150 µm hatching distance

Simple 3D extruded structures, i.e. cuboids with a size of 6x6x6 mm^3 can be seen in Fig. 3. (a). The average laser powers 100 W and 150 W, scanning speeds of 100 mm/s and 200 mm/s, hatching distances of 100 µm and 150 µm were used in this experiment. The microstructure of all samples at different parameters is shown in Fig. 3 (b) to (i). In comparison with previous work when the average laser energy is only 25 W [15], see Fig. 1. (c), the LPBF samples are much denser. All samples exhibit aligned pores corresponding to the scanning lines, especially at crossing points of vertical and horizontal scanning lines. With the average laser power of 100W, the porosity at the hatch spacing of 150 µm is higher than that at 100 µm, and the two samples at scanning speed of 200 mm/s are of higher porosity. The slower scanning contributes to longer dwell time and thus higher accumulated energy, which further contributes to better melting of the powders and denser structure after solidification. With the laser energy increasing up to 150 W, the overall porosity of the samples reduces, and the size the pores is much smaller. However, relatively bigger holes are found in the sample 150W/100mm/s/100 µm, which should be vapor holes due to the high laser energy. In order to assess density values, the surface areas of pores and melted material were calculated from the binary images. Among the eight samples, the two samples obtained at 100W/100mm/s/100 µm (Fig.3 (b)) and 150W/100mm/s/150 µm

(Fig.3 (g)) are of comparable and high densities, 96.4 % and 93.7 %, respectively. These values are significantly higher than that in the previous work when the average laser energy is only 25 W [15]. Thanks to the higher average laser power, successful melting of powder takes place and bulk bodies with less pores can be additively manufactured.

In order to demonstrate the feasibility of the process, a turbine was fabricated as an example of 3D complex structure.

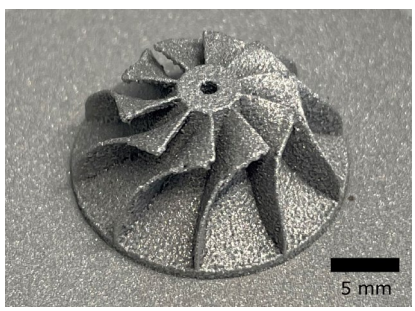

Fig 4. 3D printed turbine made of Al-Li4wt. % as a demonstration for part quality of complex structure

4. Conclusion and Outlook

In this work, laser powder bed fusion of binary Al-Li alloys has been carried out using ultrashort pulses laser. During the experiments, binary Al-Li powder with a Li content of 4 wt.% was used, which features extraordinary high stiffness and holds great potential in future lightweight construction. In comparison with our previous work [14, 15], significantly higher densities above 95% of the test bodies have been achieved by increasing the average laser power. Key element was the increase of the previously insufficient average power to values between 100 – 150 W, which allowed the generation of an increased melt pool to selectively melt the powder at the irradiated region with dramatically reduced lack of fusion effects. Furthermore, the full potential of LPBF printed Al-LI was illustrated by the fabrication of a more complex 3D structures.

In our future works, further characterizations will take place. In particular, the mechanical properties will be investigated in terms of bulk density, Young's modulus, tensile strength and hardness. Additionally, the exact amount of Li in the final product will be measured by the help of optical emission spectroscopy (OES) for different processing windows.

Acknowledgements

The authors gratefully acknowledge funding by the German Research Foundation (DFG) within the Priority Program (SPP) 2122 "Materials for Additive Manufacturing (MATframe)" (grants NO462/13-1 and Re1261/23–1).

References

[1] Santos, E.C., Shiomi, M., Osakada, K., Laoui, T., 2006. Rapid manufacturing of metal components by laser forming. International Journal of Machine Tools and Manufacture 46(12-13), p. 1459.

[2] Attaran, M., 2017. The rise of 3-D printing: The advantages of additive manufacturing over traditional manufacturing. Business Horizons 60(5), p. 677.
[3] Kruth, J.P., Froyen, L., Van Vaerenbergh, J., Mercelis, P., Rombouts, M., Lauwers B., 2004. Selective laser melting of iron-based powder. Journal of Materials Processing Technology 149(1-3), p. 616.
[4] Nie, B., Huang, H., Bai, S., Liu, J., 2015. Femtosecond laser melting and resolidifying of high-temperature powder materials. Appl. Phys. A 118, p. 37.
[5] Olakanmi, E.O., Cochrane, R.F., Dalgarno, K.W., 2015, A review on selective laser sintering/melting (SLS/SLM) of aluminium alloy powders: Processing, microstructure, and properties. Progress in Materials Science 74, p. 401.
[6] Kaden, L., Matthäus, G., Ullsperger, T., Engelhardt, H., Rettenmayr, M., Tünnermann, A., Nolte, S., 2017. Selective laser melting of copper using ultrashort laser pulses. Applied Physics A 123(9), p. 596.
[7] Ullsperger, T., Matthäus, G., Kaden, L., Engelhardt, H., Rettenmayr, M., Risse, S., Tünnermann, A., Nolte, S., 2017. Selective laser melting of hypereutectic Al-Si40-powder using ultra-short laser pulses. Applied Physics A. 123(12), p.798.
[8] Nie, B., Yang, L., Huang, H., Bai, S., Wan, P., Liu, J., 2015. Femtosecond laser additive manufacturing of iron and tungsten parts. Appl. Phys. A 119(3), p. 1075.
[9] Bauer, F., Michalowski, A., Kiedrowski, T., Nolte, S., 2015. Heat accumulation in ultra-short pulsed scanning laser ablation of metals. Opt. Express 23(2), p. 1035.
[10] Ullsperger, T., Matthäus, G., Kaden, L., Seyfarth, B., Liu, D., Rettenmayr, M., Nolte S., 2020. Laser assisted powder bed fusion of hypereutectic Al-Si using ultra-short laser pulses at different pulse durations (Conference Presentation). In Laser 3D Manufacturing VII (Vol. 11271, p. 112710M). International Society for Optics and Photonics.
[11] Ullsperger, T., Liu, D., Yürekli, B., Matthäus, G., Schade, L., Seyfarth, B., ..Nolte, S., 2021. Ultra-short pulsed laser powder bed fusion of Al-Si alloys: Impact of pulse duration and energy in comparison to continuous wave excitation. Additive Manufacturing, 102085.
[12] Noble, B., Harris, S.J., Dinsdale, K., 1982. The elastic modulus of aluminium-lithium alloys. J Mater Sci 17, p. 461.
[13] Rioja, R.J., Liu, J., 2012. The Evolution of Al-Li Base Products for Aerospace and Space Applications. Metall and Mat Trans A 43 p. 3325.
[14] Liu, D., Yürekli, B., Ullsperger, T., Matthäus, G., Schade, L., Nolte, S., Rettenmayr, M., 2021. Microstructural aspects of additive manufacturing of AlLi alloys with high Li content. Materials & Design 198, 109323.
[15] Yürekli, B., Schade, L., Ullsperger, T., Seyfarth, B., Kohl, H., Matthäus, G., ... Nolte, S., 2020. Additive manufacturing of binary Al-Li alloys. Procedia CIRP 94, p. 69.
[16] Liu, X., Du, D., Mourou, G., 1997. Laser ablation and micromachining with ultrashort laser pulses, IEEE Journal of Quantum Electronics, 33, p. 1706.